THE CHANCES OF PRECISION ENHANCE FOR ULTRASONIC IMAGING

Tomasz Rymarczyk[1,2]**, Jan Sikora**[1]**, Przemysław Adamkiewicz**[1]**, Piotr Bożek**[1]**, Michał Gołąbek**[1]
[1]Research and Development Center, Netrix S.A., Lublin, [2]University of Economics and Innovation in Lublin

Abstract. The results of ultrasonic imaging with the aid of an algorithm with the virtual rays is presented in this paper. The signal associated with the virtual rays is calculated as an arithmetical mean value of the signals of the rays surrounding the virtual one. Developed algorithm was tested on synthetic free noise data then polluted synthetic data in order to move for the real measurements. Conclusions about the imaging with new algorithm are not obvious. In same cases the significant improvement was achieved but in some not.

Keywords: ultrasound tomography, inverse problems, singular value decomposition

SZANSE NA WZROST DOKŁADNOŚCI OBRAZOWANIA ULTRADŹWIĘKOWEGO

Streszczenie. W pracy przedstawiono rezultaty działania algorytmu obrazowania ultradźwiękowego z dodatkowymi wirtualnymi promieniami. Sygnał odpowiadający wirtualnym promieniom jest wyliczany jako średnia arytmetyczna rzeczywistych sygnałów pomiarowych odpowiadających promieniom otaczącym dany promień wirtualny. Zaproponowany algorytm najpierw przetestowano na danych syntetycznych niezaszumionych, następnie na danych zaszumionych aby następnie przejść do danych pomiarowych. Wnioski na temat tego czy promienie wirtualne mają szanse podnieść jakość obrazowania nie są jednoznaczne. W niektórych przypadkach jakość jest znacznie lepsza a w innych nie.

Słowa kluczowe: tomografia ultradźwiękowa, zagadnienia odwrotne, rozkład względem wartości osobliwych

Introduction

In nonclassical tomography like Electrical Impedance Tomography (EIT) [3, 7, 15], Capacitance Tomography (CT) [18, 19], Sonic and Ultrasonic or Radio Tomography [8, 13, 14], as well as Magnetic Tomography and classical tomography [1, 2, 11, 12] always there is a lack of information. In this paper, the problem of imaging has been brought to the solution of under or over-determined system of equation. As a rule, when the spatial resolution is high (for example 64×64 pixels) than such a system of equation is under-determined for the set of 32 sensors [14]. There are many methods of the solution, but in this work, the direct solution of system of algebraic equations has been selected as a simplest and most effective one. Such an algebraic system demands the specialized method of the solution, because its condition number is very high [9]. Three different approaches have been taken into account.

The first approach depends on the solution of the under-determined system of equations with the aid of FOCUSS algorithm [4]. On the base of numerical experiments, one can say [16], that too deep under-determination of the system of equations has a bad influence on the quality of the solution. One can expect nice results if the number of unknowns is less than two times bigger than the number of observations.

The second approach is leading to a square system of equations by left side multiplication of under-determined system of equations by transposition of the coefficients matrix. However, such a multiplication rises the matrix coefficient number with the power of two. Particularly such a remark concerns the measurement data. When the coefficient number is very high than difficulties with the solution are also very high [9].

The clue of the research presented in this paper, is the third approach. The key point of this approach is such a formulation of the problem in order to, in natural way, increase the number of observations. The simplest method is to reduce the number of pixels (unknowns) in which the density function is sought. Not always reduction of pixels is acceptable. That is why the authors suggest introduction of not existing measurements so called the virtual measurements and associated with them the virtual rays.

All above mentioned cases will be illustrated and discussed in this paper.

Theoretical basis of developed algorithm interested readers could find in the monography [6]. Some interesting details are presented in the paper [16]. It is worth to stress that according to the simplifying assumptions the reflection rays will not be taken into account. That means the transmission mode of the sonic tomography will be used in this paper.

In the third case, the most interesting, from the point of view of this paper is the question, if the only way of retaining

overdetermination of the system of equations is the reduction of the pixels number?

Another way (virtual rays) of retaining over-determination of equations will be tested in this paper. Namely, artificially increasing the number of observations will be considered. The number of additional artificial observations strictly depends on the number of real sonic sensors. But the real sensors could not be increased without restraints, due to their physical size and the cost.

But some authors apply only two sensors set with the object placed on the rotating table. In that way the number of projection angles could be easily increased [10]. Certainly, not always such an approach is possible.

More projection angles, more rows of coefficient matrix. But if the number of projection angles would be too high, that could lead to linearly dependency of the rows, increasing the coefficient number and also increasing the pseudo-rank deficiency of the matrix [9].

The main goal of this paper is proposed algorithm testing with virtual rays on the real data, if the additional, artificial information are able to improve the quality of the images. As was mentioned already such an information are called the virtual information, as the sonic sensor do not exist for them. They are only in our imagination and the virtual signals are calculated on the base of the real measurements. The virtual signals are calculated as an arithmetical mean value of the surrounding ray's measurement.

Numerical experiment will be carried out in two steps. First, we will test the developed algorithm for the synthetic noise free data and next the noised data. The second part of the experiment will be carried out for real measured data. The measured data for different configurations, were obtained with the aid of the sonic tomograph design by NETRIX R&D company [8]. The reconstructions treated as the reference images were carried out with the PICUS 3 Sonic Tomograph software [5].

1. Additional, virtual ray between the real sensors – synthetic data case

One of the possibilities of enhancing the number of observations is to introduce an additional (virtual) rays between the real ones. In such a case the signal which belongs to the virtual ray will be calculated as an average value of the measurements associated with the rays surrounded the virtual one.

In this part of numerical experiment, the same number of sensors as for the real measurements was applied. The measurements were carried out by the NETRIX R&D company from Lublin [17].

In the Fig. 1 an exemplary real ray (the solid lines) and the virtual ones (dashed line) are presented. But in Fig. 2 the distribution of all rays in the region under investigation is shown.

It is worth to notice that the additional, virtual rays cause that the density of the rays inside the region is really high.

In order to be as close as possible to the real laboratory experiment the two closely placed inside objects were selected. Those objects are separated by 4 or 2 pixels as it is shown in Fig. 3. Such an example gives us a chance to investigate the proximity effect.
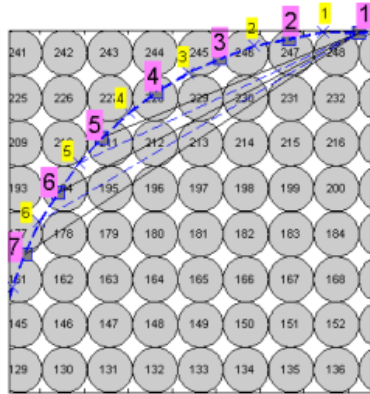

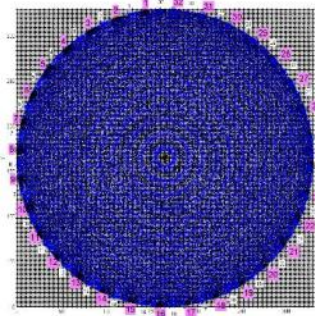*Fig. 1. Real (solid line) and additional rays (dashed line) in the region with a circular pixel*

Fig. 2. The 32 sensors on the perimetry of the region and the rays between them for 64×64 pixels discretization
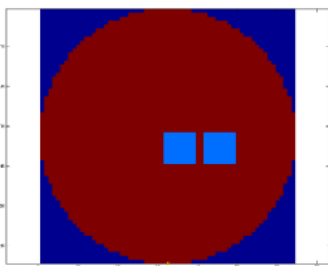

Fig. 3. Model of the region with an object inside splitted into two parts separated by gap 2 pixels wide

As a reference image (see Fig. 4) it was selected an image achieved without of additional-virtual rays with 1% noisy data for the full fan ray after median filtering.

The number of 32 sensors restrict the number of measurements which for the full fan ray is 32×31 = 992. For the spatial resolution 64×64 pixels make 4096 unknowns excluding forbidden pixels visible in the Fig. 3 and Fig. 5 as a blue or black subarea respectively.

So, the imaging problem is reduced to the solution of a generalized (underdetermined) algebraic system of equations. Because the number of observations is less over four times than the number of unknowns, so the system of equations is deeply underdetermind.

The authors experience says that the best results could be achieved when the number of unknowns is not more than two times bigger than the number of observations. In spite of that, the solution by the FOCUSS function [4] gives acceptable results as it is presented in Fig. 4.
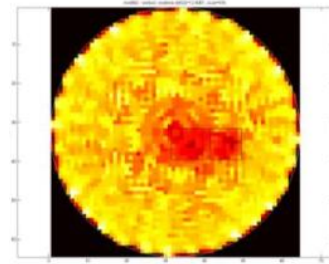

Fig. 4. Image for synthetic data with 1% noise without the virtual ray

Adding the virtual rays, the number of observations rise to 32×(31+30) = 1952, which means two times with respect of the case without of virtual rays. Reducing the ratio of unknowns to measurements by adding the virtual rays causes that the imaging produces much better results as it is shown in Fig. 5. Also, in this case the system of algebraic equations was solved by FOCUSS function and filtered by median filter [20].
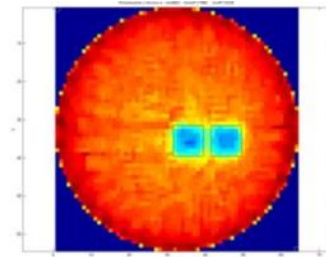

Fig. 5. Image for noise free synthetic data with virtual rays achieved by FOCUSS function
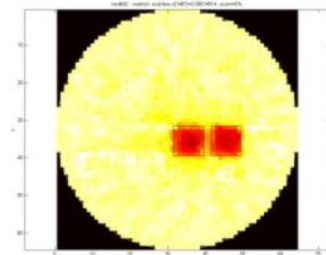

Fig. 6. Image for noise free synthetic data with virtual rays achieved by left multiplication by matrix transposition and SVD decomposition

Comparing the image in the Fig. 4 without of virtual rays with the image in Fig. 5 with the virtual rays one can justifiably say that in this particular case much better results was achieved. Such a conclusion is valid for pollution free data so far.

For the farther comparison, Fig. 6 shows the image which was achieved by left sided multiplication of a transposed coefficient matrix a well as the right-hand side vector and an application of SVD decomposition in order to get the solution. Using the left multiplication, the underdetermined system of equations became the square one. However, bed conditioned and what is more, very often rank deficient, so the solution is only possible by the decomposition method (SVD) [9].

As before, in a similar way the image was gain for synthetic noise free data using the full fan ray and filtered with the median filter. It is visible by comparison of the images in Fig. 5 and Fig. 6, the results are very similar, and is difficult to say which one is better.

Before we will pass to the real data measured in the NETRIX laboratory the algorithm was tested with the synthetic noisy data using the same object with the same obstacles inside. Results are presented in the following figures.

In Fig. 7 for the noisy synthetic data (1% of the noise) two images are presented for the separated object by four and by two pixels. Such an image maybe not ideal one could be compared with the image without the virtual rays (Fig. 4). Now for the noisy data it is not so obvious which algorithm with or without of virtual

rays is better. One thing is obvious. The virtual rays helped to see the gap between the separated obstacles. The gap is deliberately very narrow to see the influence of the proximity effect.
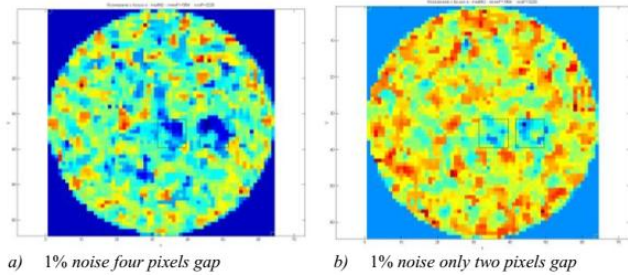

a)   1% noise four pixels gap   b)   1% noise only two pixels gap

Fig. 7. Images for the noisy synthetic observations

From the other side the background of the image without of virtual rays is calmer what is an obvious advantage.

Conclusion: in case of synthetic data virtualization of rays has some sense. However, their influence on the quality of image, particularly for the noisy data is a little disappointed.

The more vital will be behaviour of the proposed algorithm for the real data which will be presented in the next sections of this paper.

2. Additional, virtual ray between the real sensors – measured data case

Research of influence of virtual rays on the quality of imaging using the synthetic noise free data allow for a bit of optimism. It is not so optimistic as we applied the noisy data. That is why the next step with real life laboratory data will be investigated. Then, could be answered the main question if the virtual rays help improve the quality of the sonic images or do not. The three following cases will be considered.

The first case: three objects – excitation frequency 48 kHz

The measuring set up for the first case is shown in Fig. 8. The arrangement consists of three bottles filled out with an air. One of the bottles is placed in the geometrical centre of the region, where the sensitivity is the smallest. The frequency of excitation is 48 kHz.

Fig. 8. Setup for ultrasonic measurements with the aid of NETRIX tomograph

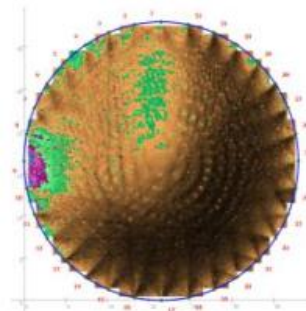*Fig. 9. Three objects inside the region filled with water*

Fig. 10. Reconstruction with the aid of PICUS 3 software [5]

The Phantom of the region is presented in Fig. 9 and the image reconstruction with the aid of software of the Tomograph PICUS 3 [5] is shown in Fig. 10. This image would be treated as a reference image. It is easy to notice that the obstacle in the centre of the region has the worse representation in the reference picture.

The images obtained with the aid of the algorithm with additional virtual rays are presented in the following figures. Images were obtained by three different methods which were described above, for two different spatial resolution: 32×32 pixels and 64×64 pixels.
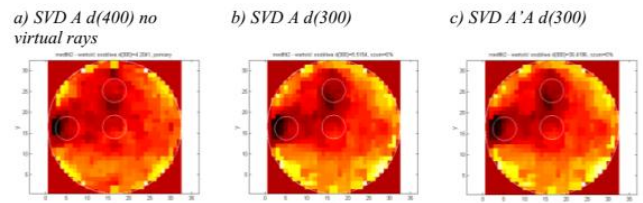

a) SVD A d(400) no virtual rays   b) SVD A d(300)   c) SVD A'A d(300)

Fig.11. Imaging of the three objects based on laboratory measurements

For the spatial resolution 32×32 pixels in Fig. 11a without of virtual rays and Fig. 11b with virtual rays for different number of singular values were constructed the trial solutions. In Fig. 11c the solution was achieved by left sided multiplication by the coefficients matrix transposition (A'A, where A' means A^T in MATLAB nomenclature [20]).

The differences in the images it is difficult to distinguish. Similarly, to the reference image, the central obstacle is not distinctly represented.
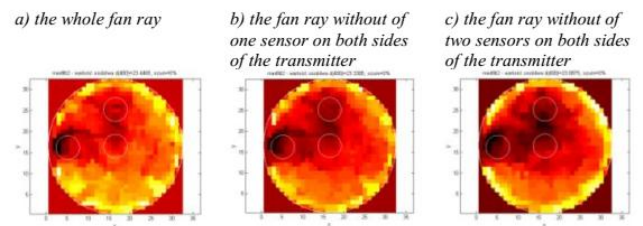

a) the whole fan ray   b) the fan ray without of one sensor on both sides of the transmitter   c) the fan ray without of two sensors on both sides of the transmitter

Fig. 12. Influence of the beam width on the imagining

The influence of the wideness of the fun ray on the quality of the image is presented in Fig. 12. The image for the whole fan ray is shown in Fig. 12a. For a narrower fan ray without one sensor on both side of the transmitter is shown in Fig. 12b and slightly narrower the fan ray without of two sensors on both sides of the transmitter in Fig. 12c. As one can see from those images the narrower ray produces slightly better results.

It could be explained by the following fact. The adjacent sensors have the measurements with the highest relative error due to their shortest distance between them. If such measurements would be excluded than the quality of data increase resulting with nicer images.
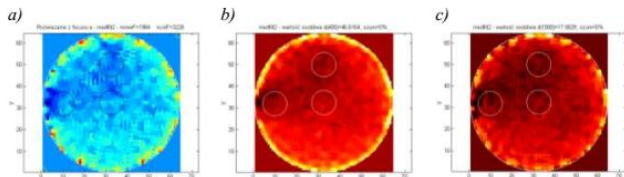
Fig. 13. Images after 2-D median filtering process: a) underdetermined system of equation by FOCUSS, b) SVD solution for the first 400 singular values, c) SVD solution for the first 928 singular values (A'A)

Increasing the spatial resolution do not enhance the quality of the images, as could be observed in Fig. 13. For the same number of observations, the number of unknowns become higher, leading to far worse underdetermination of algebraic system of equations.

The Fig. 13a shows the image obtained by underdetermined system solution. One can see that something happened in the second quarter of the region. A slightly better result was achieved by the solution of the square system of equations for the first 400 singular values and then for 928. As one can see increasing more than two times the number of singular values does not help much (consult Fig. 13c).

The only way to enhance the quality of an image is increasing the number of observations by generating non-existent virtual rays.

The second case: four objects – excitation frequency 48 kHz

As a second case the four internal objects located as it is shown in Fig. 14 has been considered. The next Fig. 15 illustrates the reconstruction results. As before the object placed in the centre of the region has the weakest representation. This image will be a reference one in our experiment.
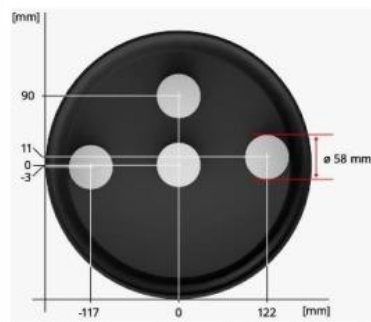

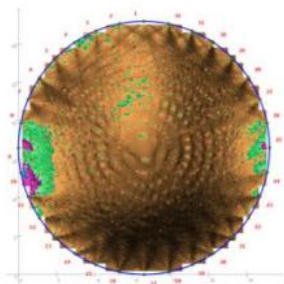*Fig. 14. Four objects inside the region filled with water*

Fig. 15. Reconstruction with the aid of PICUS 3 software [5]

Reconstruction of the four distributed objects are presented in Fig. 16. In Fig. 16a and Fig. 16b the spatial resolution was 32×32 pixels but in Fig. 16c increased up to 64×64. For 32 sensors the lower spatial resolution guarantee overdetermination of the system of algebraic equations. One has got slightly more observations than the unknowns for such spatial resolution. The forbidden pixels inside of the square region which lay outside the circular region are not treated as unknown values. In Fig. 16a image was reconstructed without of virtual rays but in Fig. 16b with the virtual rays. It is very hard to judge which one is better.

The authors would like to believe that the second one, because it poses more tranquil background. Increasing the spatial resolution to 64×64 pixels the image deteriorates as it was in previous case (Fig. 13a). Explanation of this phenomenon remain the same.
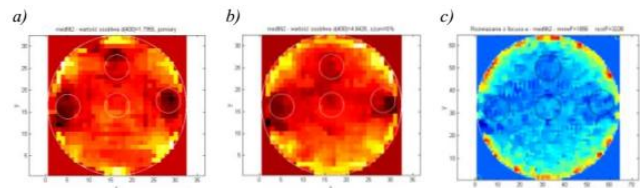

Fig. 16. Reconstruction for the four objects: a) without of virtual rays A d (400), b) with the virtual rays for 32×32 spatial resolution (overdetermined system of equations SVD – A d (400), c) the same case as in b-case but spatial resolution increased to 64×64 driven to underdetermined system of equations solved by FOCUSS

So again, raises the question if for such a number of sensors better resolution is justified as it leads for worse imaging results?

In this case the left side multiplication by the transposition of the coefficient matrix are able to improve a little bit the image but under condition that the number of singular values for trial solution would be properly chosen. In Fig. 17 we can observe the distribution of singular values. At a first glance 500 singular values seems to be the correct one. But in the range of 400 till 500 singular values the curve goes down rapidly. We have to remember that the vertical axis is in a logarithmic scale, so within this range the singular values decreasing significantly. The best results were achieved not for 500 but for 150 singular values (see Fig. 18).
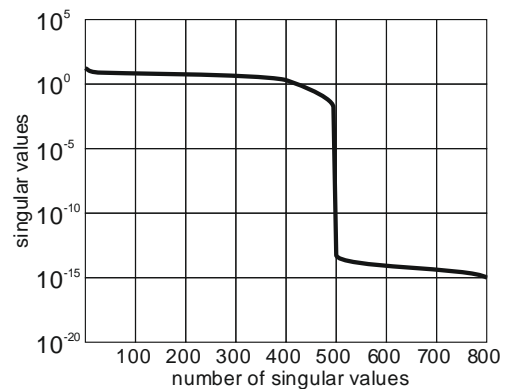

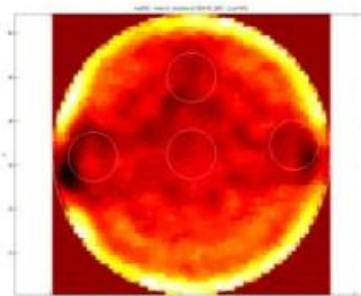*Fig. 17. Singular values distribution*

Fig. 18. Image for the four objects and resolution is 64×64 SVD A'A d(150)

The background is calm, and it is an easy to detect the trace of the internal objects, however with a small offset. The problems with the central object remained.

As a general remark in case of measurements is that one has to select the trial solution with a reasonable condition number. It is very hard to define the "reasonable" condition number. It depends on the case considered. By the numerical experiments the authors think that it is rather the dozens but definitely not the thousands.

—————— IAPGOŚ 3/2018 ——————

For the four bottles case the condition number for jump of the singular values is d(1)/d(496) = 1231.7 (consult the Fig. 17). For such a number of singular values the trial solution produces a low-quality image. That is why finally only 150 singular values were selected what gives the condition number equal only 10.58. The results are visible in Fig. 18.

Comparing this result with the reference image (Fig. 15) there is no the central object and also the object placed vertically over the central one has also a very week representation.

The third case: four objects – excitation frequency 400 kHz

As the last experiment the four a smaller than in previous cases, bottles filled in air for excitation of 400 kHz was selected.
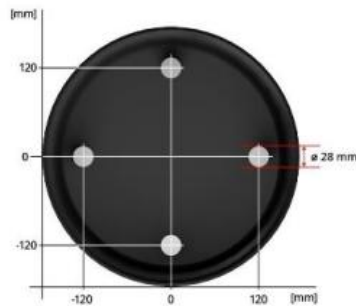

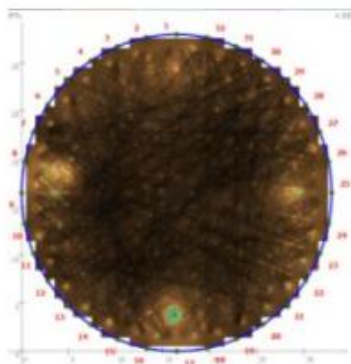*Fig. 19. Four objects location inside the region filled with the water*

Fig. 20. Reconstruction with the aid of PICUS 3 software [5]

The configuration of internal obstacles is presented in Fig. 19. In spite of that the smaller object is more difficult to identify the reference image is very good. Again, the question is if the proposed algorithm with the virtual rays would be able to produce reasonable image equally good as the reference one.

This time the images are presented in the highest resolution 64×64 pixels. In the Fig. 21 the upper row is showing the raw images but the lower row images after median filtering.
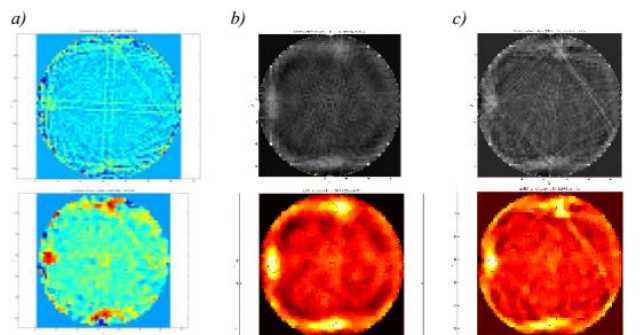

Fig. 21. Images for the virtual rays and four objects from the Fig. 19; upper row the raw images but the lower row images after 2D median filtering a) FOCUSS b) SVD A'A – d(100) c) SVD A'A – d (300)

In the Fig. 21a the image from the solution of under-determined system of equations is shown but the Fig. 21b and Fig. 21c presents the images from the SVD solution for different number of singular values achieved after left side multiplication by transposition of the coefficient matrix.

It is worth to notice that one of the internal objects in the reference image is weaker than the rest ones. For our method as it is seen in Fig. 21, this one is hardly visible at all.

Enlarging the number of singular values does not improve the image (Fig. 22a). So far only the median filtering was applied. But if the image was treated by adaptive Wiener filter [20] we can observe an improvement of the image. Now all four internal objects are visible (see Fig. 22b).
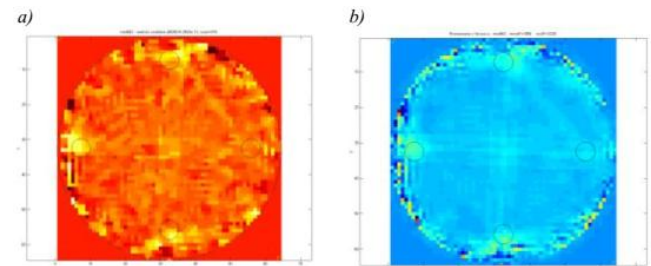

Fig. 22. Image for the four objects from the Fig. 19: a) SVD A'A – d (500), b) FOCUSS filtered with the aid of the adaptive Wiener method [20]

3. Conclusion

In this paper a new method for sonic imaging with virtual rays was presented. Algorithm tested on synthetic noise free data shows significant improvement when the virtual rays were engaged.

However noised data reveal sensitivity of the new algorithm on the noisy data. Merely 1% noise was able to distort significantly the image.

That was not good perspective for the real application of the algorithm. So, the most important was the behaviour of the proposed algorithm in the second part of experiment, with the real data.

The results are not as obvious and not unambiguous as one could expect. For some experiment, improvement could be visible but for the other rather not.

That is why, according the authors opinion, this algorithm based on a very strong simplifying assumptions like for example not taking into account reflecting signals, has reached the end of its ability.

The further sonic imaging improvement could be reached due to relaxing some of the strongest simplifying assumptions.

It will depend on the ability of the measurement, if we would be able to measure the reflecting signals inside the region. Such an ability allows to move from the transition mode to the reflecting mode. Authors believe that it helps to get much more precise images.

References

[1] Bartušek K., Fiala P., Mikulka J.: Numerical Modeling of Magnetic Field Deformation as Related to Susceptibility Measured with an MR System. Radioengineering 17(2)/2008, 113–118.

[2] Bartušek K., Drexler P., Fiala P. et al.: Magnetoinductive Lens for Experimental Mid-field MR Tomograph. Progress in Electromagnetics Research Symposium Location: Cambridge 2010, 1047–1050.

[3] Dušek J., Hladký D., Mikulka J.: Electrical Impedance Tomography Methods and Algorithms Processed with a GPU. PIERS Proceedings (Spring) 2017, 1710–1714.

[4] Gorodinitsky I.F., George J.S., Rao B.D.: Neuromagnetic source imaging with FOCUSS: a recursive weighted minimum norm algorithm. Clinical Neurophysiology 95/1995, 231–251.

[5] Göcke L: PiCUS Sonic Tomograph Software Manual, Argus Electronic Gmbh, Erich-Schlesinger-Straße 49d, 18059 Rostock, Germany, 2017, www.argus-electronic.de.

[6] Kak A.C., Slaney M.: Principles of Computerized Tomographic Imaging. IEEE Press, New York 1999.

[7] Kłosowski G., Rymarczyk T.: Using Neural Networks and Deep Learning Algorithms in Elecrical Impedance Tomography. Informatyka, Automatyka Pomiary w Gospodarce i Ochronie Środowiska (IAPGOŚ) 3/2017, 99–102.

[8] Koulountzios P., Rymarczyk T., Soleimani M.: Ultrasonic Tomography for automated material inspection in liquid masses. 9th World Congress on Industrial Process Tomography, Bath, Great Britain, 2–6 September 2018.

[9] Lawson Ch.L., Hanson R.J.: Solving Least Squares Problems. Classics in Applied Mathematics 15/1998.

[10] Łopato P.: Detekcja i identyfikacja defektów struktur dielektrycznych i kompozytowych z wykorzystaniem fal elektromagnetycznych w zakresie terahercowym. Wydawnictwo Uczelniane Zachodniopomorskiego Uniwersytetu Technologicznego w Szczecinie, Szczecin 2018.

[11] Marcon P. et al.: Magnetic susceptibility measurement using 2D magnetic resonance imaging. Measurement Science and Technology, 2011, 22.10: 105702.

[12] Mikulka J.: GPU–Accelerated Reconstruction of T2 Maps in Magnetic Resonance Imaging. Measurement Science Review 4/2015, 210–218.

[13] Yang M., Schlaberg H.I., Hoyle B.S., Beck M.S., Lenn C.: Real-Time Ultrasound Process Tomography for Two-Phase Flow Imaging Using a Reduced Number of Transducers. IEEE Transactions on Ultrasonics, Ferroelectrics and Frequency Control 46(3)/1999.

[14] Polakowski K., Filipowicz S.F., Sikora J., Rymarczyk T.: Quality of imaging in multipath tomography. Przeglad Elektrotechniczny 85(12)/2009, 134–136.

[15] Rymarczyk T., Sikora J., Waleska B.: Coupled Boundary Element Method and Level Set Function for Solving Inverse Problem in EIT. 7th World Congress on Industrial Process Tomography WCIPT7 2013, 312–319.

[16] Rymarczyk T., Sikora J., Polakowski K., Adamkiewicz P.: Efektywny algorytm obrazowania w tomografii ultradźwiękowej i radiowej dla zagadnień dwuwymiarowych. Przegląd Elektrotechniczny 94(6)/2018.

[17] Rymarczyk T. et al.: Sposób i układ do prowadzenia pomiarów w elektrycznej tomografii pojemnościowej. Zgłoszenie patentowe P.418304 z dnia 12.08.2016.

[18] Smolik W.: Forward Problem Solver for Image Reconstruction by Nonlinear Optimization in Electrical Capacitance Tomography. Flow Measurement and Instrumentation 21/2010, 70–77.

[19] Soleimani M., Mitchell C.N., Banasiak R., Wajman R., Adler A.: Four-dimensional electrical capacitance tomography imaging using experimental data. Progress in Electromagnetics Research 90/2009, 171–186.

[20] http://www.mathworks.com/products/matlab/ (June 2018).

Ph.D. Eng. Tomasz Rymarczyk
e-mail: tomasz@rymarczyk.com

He is the director in Research and Development Center in Netrix S.A. and the director of the Institute of Computer Science and Innovative Technologies in the University of Economics and Innovation, Lublin, Poland. He worked in many companies and institutes developing innovative projects and managing teams of employees. His research area focuses on the application of non-invasive imaging techniques, electrical tomography, image reconstruction, numerical modelling, image processing and analysis, process tomography, software engineering, knowledge engineering, artificial intelligence and computer measurement systems.

Prof. Jan Sikora
e-mail: sik59@wp.pl

Prof. Jan Sikora (PhD. DSc. Eng.) graduated from Warsaw University of Technology Faculty of Electrical Engineering. During 44 years of professional work he has proceeded all grades, including the position of full professor at his alma mater. Since 1998 he has worked for the Institute of Electrical Engineering in Warsaw. In 2008, he joined Electrical Engineering and Computer Science Faculty in Lublin University of Technology. During 2001-2004 he has worked as a Senior Research Fellow at University College London in the prof. S. Arridge's Group of Optical Tomography.

Ph.D. Przemysław Adamkiewicz
e-mail: p.adamkiewicz@netrix.com.pl

He is a doctor of physics, graduate of Maria Curie-Sklodowska University in Lublin. He is a head of the R&D Department at Netrix S.A. His research area focuses on electrical impedance tomography, electrical capacitance tomography, image reconstruction, forward problem, inverse problem, numerical modelling, image analysis and computer measurement systems.

M.Sc. Eng. Piotr Bożek
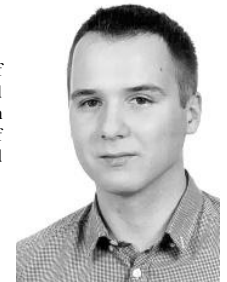e-mail: piotr.bozek@netrix.com.pl

Piotr Bożek is graduated form Lublin University of Technology, faculty of Electrical Engineering and Computer Science (Specialty: Intelligent Technologies in Electrical Engineering). Currently is working on projects of computerized tomography in the NETRIX S.A. Research and Development Center.

M.Sc. Eng. Michał Gołąbek
e-mail: michal.golabek@netrix.com.pl

Michał Gołąbek is graduated form Lublin University of Technology, faculty of Electrical Engineering and Computer Science (Specialty: microprocessor Drives in industrial automation). At present he is constructor of tomographic equipment in NETRIX S.A. Research and Development Center.